Frontal belt curvature and oblique ramp development at an obliquely collided irregular margin: Geometry and kinematics of the NW Taiwan fold-thrust belt

Olivier Lacombe, Frédéric Mouthereau, and Jacques Angelier

Laboratoire de Tectonique, UMR 7072, Université P. et M. Curie, Paris, France

Hao-Tsu Chu

Central Geological Survey, Taipei, Taiwan

Jian-Cheng Lee

Institute of Earth Sciences, Academia Sinica, Taipei, Taiwan

Received 8 July 2002; revised 22 October 2002; accepted 26 February 2003; published 24 June 2003.

[1] Combined structural and tectonic analyses demonstrate that the NW Foothills of the Taiwan collision belt constitute mainly an asymmetric "primary arc" type fold-thrust belt. The arcuate belt developed as a basin-controlled salient in the portion of the foreland basin that was initially thicker, due to the presence of a precollisional depocenter (the Taihsi basin). Additional but limited buttress effects at end points related to interaction with foreland basement highs (Kuanyin and Peikang highs) may have also slightly enhanced curvature. The complex structural pattern results from the interaction between low-angle thrusting related to shallow decollement tectonics and oblique inversion of extensional structures of the margin on the southern edge of the Kuanyin basement high. The tectonic regimes and mechanisms revealed by the pattern of paleostress indicators such as striated outcrop-scale faults are combined with the orientation and geometry of offshore and onshore regional faults in order to accurately define the Quaternary kinematics of the propagating units. The kinematics of this curved range is mainly controlled by distributed transpressional wrenching along the southern edge of the Kuanyin high, leading to the development of a regional-scale oblique ramp, the Kuanyin transfer fault zone, which is conjugate of the NW trending Pakua transfer fault zone north of the Peikang basement high. The divergence between the N120° regional transport direction and the maximum compressive trend that evolved from N120° to N150° (and even to N–S) in the northern part of the arc effectively supports distributed wrench deformation along its northern limb during the Pleistocene. The geometry and kinematics of the western Taiwan Foothills therefore appear to be highly influenced by both the preorogenic structural pattern of the irregularly shaped Chinese passive margin and the obliquity of its Plio-Quaternary collision with the Philippine Sea plate. *INDEX TERMS:* 8102 Tectonophysics: Continental contractional orogenic belts; 8010 Structural Geology: Fractures and faults; 8005 Structural Geology: Folds and folding; 8164 Tectonophysics: Stresses—crust and lithosphere; 9320 Information Related to Geographic Region: Asia; *KEYWORDS:* tectonics, oblique inversion, arcuate belt, Taiwan, basin-controlled salient. **Citation:** Lacombe, O., F. Mouthereau, J. Angelier, H.-T. Chu, and J.-C. Lee, Frontal belt curvature and oblique ramp development at an obliquely collided irregular margin: Geometry and kinematics of the NW Taiwan fold-thrust belt, *Tectonics*, *22*(3), 1025, doi:10.1029/2002TC001436, 2003.

0278-7407/03/2002TC001436$12.00

1. Introduction and Scope of the Study

[2] The active fold-thrust belt of western Taiwan (Figure 1) results from the oblique collision of the Philippine Sea plate (the Luzon arc) with the Eurasian Plate (the Chinese passive margin) since 6.5–5 Ma [e.g., *Suppe*, 1981; *Teng*, 1990]. The Taiwan fold-thrust belt developed as a growing sedimentary wedge prograding onto the Chinese passive margin in response to the N310° relative convergence between the Philippine Sea plate and Eurasia [*Seno et al.*, 1993]. An initial submarine accretionary stage occurred mainly around 5 Ma coeval with the beginning of the flexural subsidence of the Eurasian lithosphere [*Mouthereau et al.*, 2001]. It was followed between 2 and 1 Ma by the filling of the foreland basin, the rapid increase in accumulation rates [*Chang and Chi*, 1983; *Teng*, 1990] reflecting the exhumation and the subsequent denudation of the Central Range. The last stage began at around 1 Ma, and the outermost thrusts were activated at that time, incorporating within the wedge the syntectonic deposits of the foreland basin.

[3] *Lu and Malavieille* [1994] performed 3D sandbox models of the oblique collision of a deformable medium (the Chinese passive margin) by an asymmetrical indenter (the Luzon arc belonging to the Philippine Sea plate) to

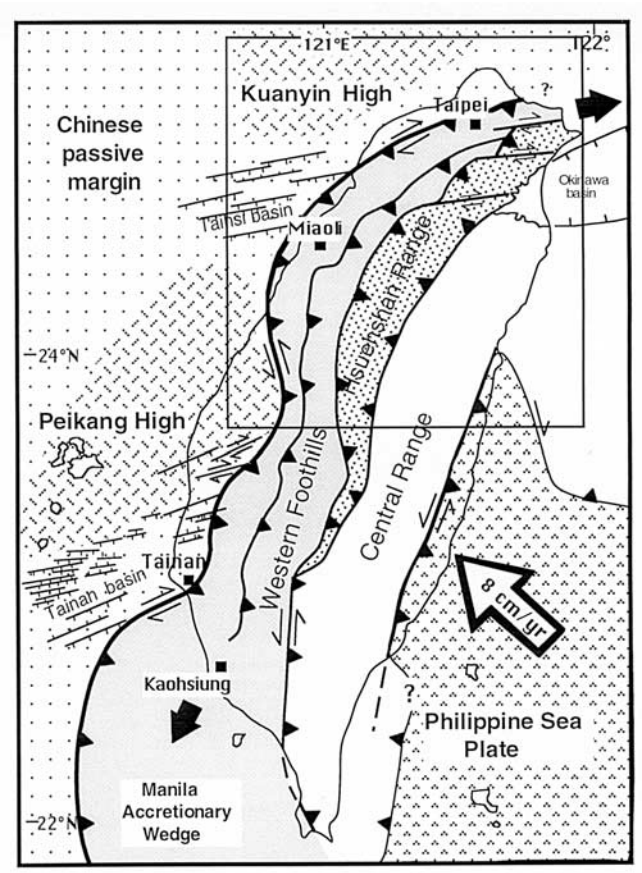

Figure 1. Tectonic setting and main structural features of Taiwan. The large open arrow shows the direction of convergence of the Philippine Sea plate relative to the Chinese passive margin. Heavy lines indicate major thrusts, triangles on upthrown side; lines with double arrows indicate wrench faults. The gray pattern represents the Foothills. Hatched areas correspond to basement highs of the Chinese margin underlying the deposits of the foreland basin. Black arrows indicate tectonic escape at the tips of the belt. The frame shows the investigated area.

simulate the Taiwan thrust wedge development and kinematics. The modeling results account for the overall structure of the Taiwan mountain belt but fail to reproduce the regional ''S'' shape of the outermost units of the belt (Figure 1). Because the collided Chinese margin displays a succession of basement highs and basins inherited from its Paleogene to Miocene extensional history, namely from north to south the Kuanyin high, the Taihsi basin, the Peikang high and the Tainan basin (Figures 1 and 2; section 3), and since foreland deformation is known to be largely influenced by the irregular shape of the collided margin [e.g., *Sengör*, 1976], further sandbox modeling has attempted to simulate the influence of such rheological heterogeneities on thrust propagation during collision [*Lu et al.*, 1998]. The main result of this modeling is that the general shape of the Taiwan Foothills results from both the oblique impingement of the growing wedge by an asymmetric hinterland indenter and the development of this wedge onto the irregularly shaped Chinese margin displaying a pair of prominent basement highs which behave as buttresses and localize contraction in front of them.

[4] In NW Taiwan, the fold-thrust belt front displays a large-scale curvature, swinging a full 90° angle from a N160° direction in the south to a N070° direction in the north (and even N080° at its easternmost tip) and forms a salient (Figure 2). In the light of the sandbox modeling by *Lu et al.* [1998], this salient appears to be mainly the result of the interaction of the growing wedge with the Kuanyin and Peikang structural highs in the foreland, the thrust sheets forming the salient being free to propagate westwards between the basement obstacles. However, the NW Taiwan arcuate belt has received poor attention up to now; not only has the influence of the basement on the development of the arcuate belt in terms of variations along the strike of the belt of the preorogenic sediment thickness or the reactivation of inherited basement faults never been investigated, but the actual kinematics of the belt is poorly known. As a consequence, it has been until now very difficult to discuss whether the curvature was achieved right from the beginning of wedge development or if the belt was initially straight and underwent oroclinal bending because of its interaction with the basement obstacles of the foreland acting as buttresses, or both (section 2).

[5] This paper analyzes the geometry and kinematics of the NW Taiwan arcuate belt which developed between the Peikang and Kuanyin highs (Figure 1). It aims at showing that the arcuate shape of the salient was mainly achieved at the beginning of the formation of the wedge (primary arc) and was largely controlled by the preorogenic structural pattern of the irregular Chinese margin, that is by both the preorogenic variations in thickness of the sediments and the pattern of preorogenic normal faults which underwent transpressional reactivation on the southern edge of the Kuanyin basement high and guided emplacement of thrust sheets. To this respect, we carried out an analysis of the geometry and kinematics of regional faults and combine it with an extensive study of paleostress indicators such as outcrop-scale striated faults in order to constrain the Quaternary tectonic mechanisms; this will allow to propose a coherent tectonic and kinematic scenario for the development of the Taiwan NW fold-thrust belt.

2. Models of Salient Development and Possible Scenarios for the Development of the NW Taiwan Arcuate Fold-Thrust Belt

[6] Arcuate mountain belts have been recognized and described in many regions throughout the world (e.g., Western Alps, Jura Mountains, Iberian Arc, Appalachians, Idaho–Wyoming belt in the Rockies, Carpathians). Extensive reviews of the geometry and models of development of fold-thrust belt salients have recently been proposed. On the basis of geometrical analysis of numerous salients worldwide coupled with sandbox modeling, *Macedo and Marshak* [1999] investigated the signature in terms of

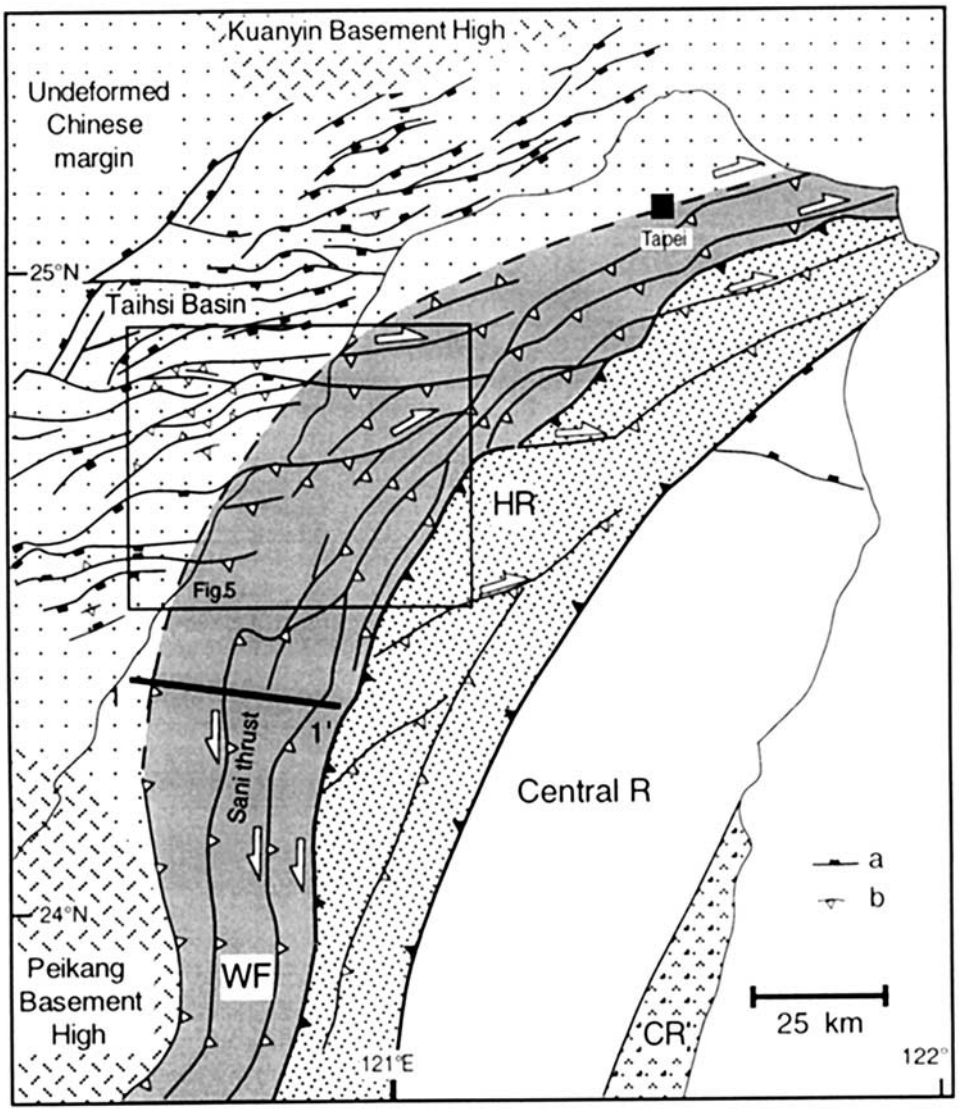

Figure 2. Structural map of the NW Taiwan fold-thrust belt and the adjacent offshore Chinese passive margin. WF: Western Foothills; HR: Hsuehshan Range, Central R.: Central Range, CR: Coastal Range. Offshore fault pattern: a: normal fault; b: inverted normal fault. 1-1′: Cross section of Figure 6.

map-view shape, symmetry and structural patterns of different scenarios of salient development, including indenter-controlled salients (the geometry of which reflects interaction of a fold-thrust belt with an hinterland indenter), basin-controlled salients (the geometry of which reflects lateral variations in the thickness of predeformational basin fill) and detachment-controlled salients (the geometry of which reflects lateral variations in the strength of the detachment surface).

[7] From a more genetic point of view, *Hindle and Burkhard* [1999] propose that three end-member cases describe most arc geometries. The ''orocline'' type results from the secondary bending of an initially straight fold-thrust belt when the belt is emplaced onto salients and recesses of the foreland during final stages of collision [*Carey*, 1955]. The ''Piedmont glacier'' type displays radial thrusting [*Merle*, 1989] associated with radially divergent transport directions: gravity sliding induced by body forces within a thrust wedge [*Platt et al.*, 1989] may lead to this type. In the ''primary arc'' type, the arcuate shape is achieved from the beginning of its formation; lateral variations in facies, thickness and/or irregularities in the foreland (e.g., basement promontories) are potential sources for curvature development [*Marshak et al.*, 1992; *Ferrill and Groshong*, 1993]. This primary arc type, documented for instance in the Jura mountains [*Hindle and Burkhard*, 1999], typically shows divergent finite strain trajectories contrasting with the nearly uniform displacement field.

[8] Taking into account the tectonic setting of Taiwan, possible scenarios for the development of the NW Taiwan arc include basin-controlled salient (1), indenter-controlled salient (2) (both may correspond to a primary arc if the

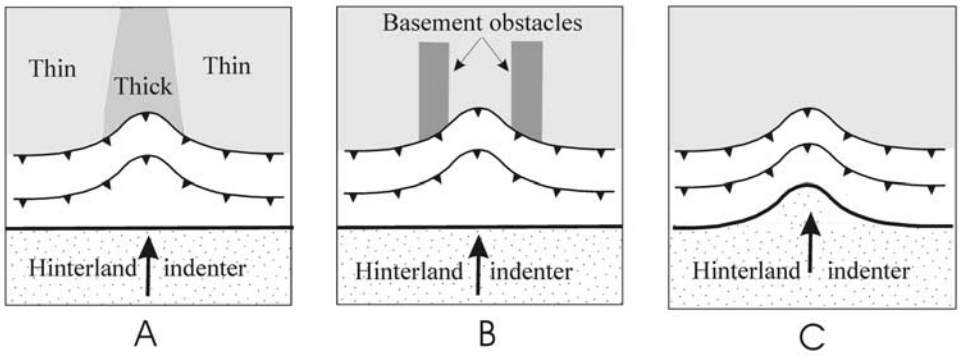

Figure 3. Possible scenarios of salient development of the NW Taiwan arcuate belt: (a) basin-controlled salient; (b) interaction with foreland (basement) obstacles; (c) indenter-controlled salient.

indenter moves with a uniform direction), interaction with basement obstacles within the foreland which may either remain limited to the end points of the arc and result only in local guidance of thrust orientation by basement faults (3) or lead to clear oroclinal bending (4) (Figure 3). Deciphering the kinematics of the NW Taiwan fold-thrust belt and choosing between different possible scenarios therefore require the analysis of the geometry of the arcuate belt, its relationships with the preorogenic structural pattern, and characterization of both the finite strain-paleostress patterns and displacement field within the arc.

3. Evidence of Basement Control on Development of the Arcuate Belt in NW Taiwan: Along-Strike Variations of Preorogenic Sediment Thickness

[9] The foreland of the Taiwan thrust belt, i.e., the Chinese platform and the Taiwan Coastal Plain, displays numerous preorogenic Tertiary basins. Among them, Paleogene and Neogene basins are distinguished on the basis of a widespread early Miocene unconformity [*Sun*, 1982]. The first type developed in response to stretching of the Eurasian lithosphere that led to the opening of the South China Sea during the Oligocene to the early Miocene. The resulting Paleogene extensional basins trend northeast and are filled with shelf sediments, tuffs, and lava flows revealing the volcanic activity at this time. Extensional tectonism continued to the early Neogene, but changes of stretching directions occurred with time as revealed by the geodynamic reconstructions and microtectonic data [e.g., *Angelier et al.*, 1990a]. This period of rifting resulted in the development of a series of northeast trending horsts and grabens, overprinting the Paleogene basins. Miocene formations mainly consist of a few kilometers of alternating shales and sandstones deposited in a shallow marine environment.

[10] The Taiwan orogen developed mainly since 6.5–5 Ma, the time of the beginning of the flexural subsidence in the foreland [*Chang and Chi*, 1983; *Lin and Watts*, 2002]. The resulting foredeep basins strike N10°–20°E, nearly perpendicular to the direction of convergence and are superimposed onto the precollisional basins. These basins migrated toward the outer part of the belt and were progressively filled in with synorogenic deposits. These synorogenic deposits are composed of the thick sequence of the Chinshui, Cholan, and Toukoshan formations. The transgressive sequence of Chinshui shales represent an important rise of relative sea level contemporaneous with the onset of foreland flexural subsidence. Above, the sandstones and shales of the Cholan formation and the Toukoshan conglomerates outline the progressive evolution from a shallow marine to a fluviatile depositional environment corresponding to a basin-scale regressive sequence coeval with the infilling of the foreland basin.

[11] The contour map of the pre-Miocene rocks of Figure 4a is based on data collected in the literature for 70 onshore and offshore wells [*Chou*, 1971, 1980; *Shaw*, 1996; *Mouthereau et al.*, 2002]. We especially consider the basins and highs, both onshore (Coastal Plain) and offshore (Taiwan Strait). The basement map clearly highlights the occurrence of two major intrabasinal highs underlying the Taiwan Strait and the Coastal Plain: the offshore Kuanyin high to the north and the partly onshore Peikang high in central western Taiwan (Figure 4a). In order to characterize the basement topography beneath the foreland and the location of Tertiary basins, we have constructed a longitudinal stratigraphic profile (Figure 4b) based on the available wells drilled in the Coastal Plain and the outer part of the Western Foothills. This profile has been constructed to fit with the relevant wells rather than considering the orientation of the normal faults that define the basins. This profile clearly emphasizes along-strike variations of basement depth and thickness of Neogene deposits (Figure 4).

[12] The transitions between highs and basins are marked by major boundary faults [*Mouthereau et al.*, 2002]; some of them have been recognized in the cover as major transfer fault zones, e.g., the Pakua transfer fault zone (PTFZ [*Deffontaines et al.*, 1997; *Mouthereau et al.*, 1999]). In the area investigated, the precollisional Taihsi Basin, located on the southern edge of the Kuanyin structural high, deserves attention. As revealed by Figure 4, it corresponds to the northern Miocene depocenter. Both the pre-Miocene basement of the Taihsi Basin and the entire overlying Neogene sedimentary cover have been uplifted. The seismic

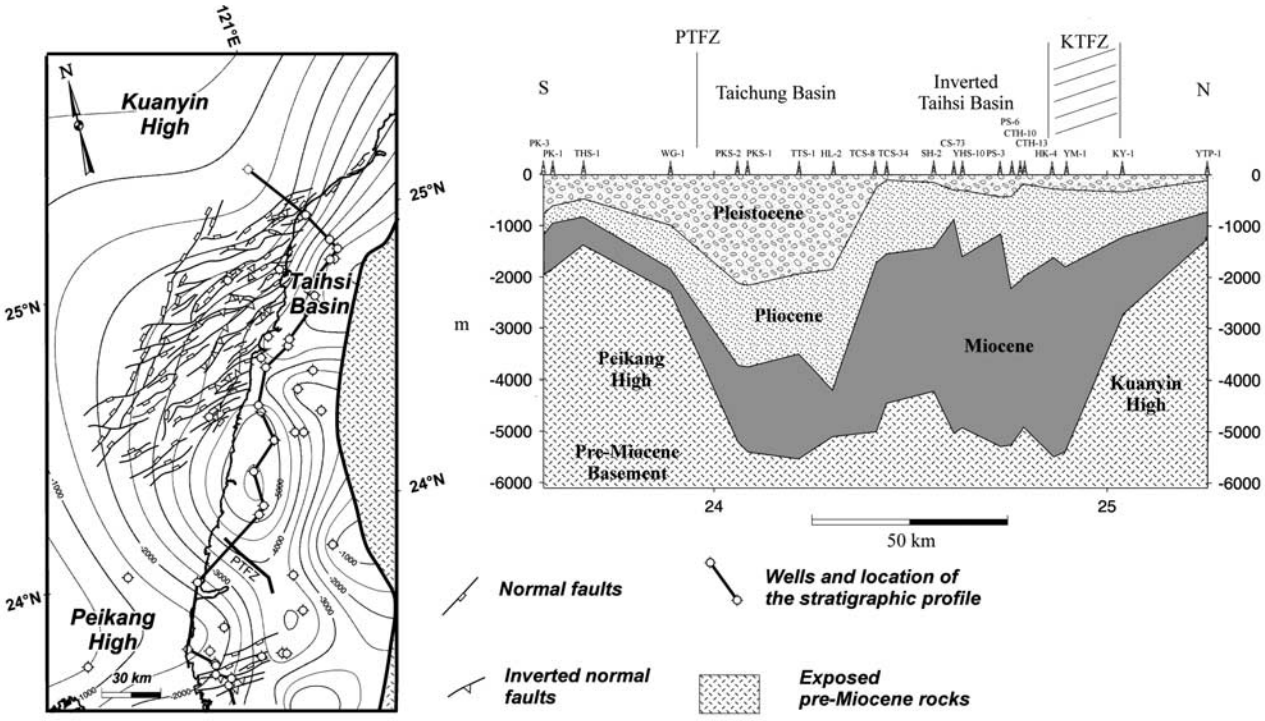

Figure 4. (a) Contoured map of pre-Miocene rocks (''basement'') and main structural pattern of offshore Taiwan. Contour interval is 500 m. PTFZ-Pakua transfer-fault zone, KTFZ-Kuanyin transfer fault zone discussed in the present work. (b) Along-strike stratigraphic profile of the Taiwan foreland showing the location of basins and highs. Note the major basement highs (Kuanyin high and Peikang high) and the inverted Taihsi Basin located on the southern edge of the Kuanyin high. The Pakua transfer fault zone delineates the Peikang high from the northern Paleogene-Neogene basins (Taichung and Taihsi basins).

studies of the geologists of the Chinese Petroleum Corporation have extensively demonstrated that the Taihsi Basin is an inverted basin [*Huang et al.*, 1993; *Shen et al.*, 1996]. The Neogene Taichung Basin shows important foredeep subsidence as suggested by the thick series of syntectonic deposits of continental origin. Its development appears to have been also controlled by a major oblique transfer fault located north of the Peikang high, the Pakua transfer fault zone, an ancient normal fault that locally controlled the propagation and geometry of frontal thrust sheets [*Mouthereau et al.*, 1999].

[13] The pattern of folds and west verging imbricate thin-skinned thrust sheets of the arcuate fold-thrust belt of NW Taiwan formed in relation with various decollement levels recognized within both the precollisional Paleogene to Miocene deposits or the synorogenic Plio-Pleistocene formations on the basis of their geometric relationships with main thrusts and by the additional support of seismic reflection data (Figures 5 and 6). The arc clearly developed in the portion of the foreland basin that was initially thicker (the Taihsi basin). In map view, fold trends and thrust strikes converge toward the end point, in agreement with the lateral thinning of the sedimentary sequence involved in thrusting toward the end points, while the position of the salient's apex coincides with the location of the precollisional depocenter (thickest strata) in the basin from which the salient formed. In addition, the largest thrust spacing occurs at the salient apex, in agreement with sandbox modeling of thin-skinned thrust wedges. This demonstrates the control on the development of the NW Taiwan salient exerted by the distribution of the basement highs and the related along-strike variation in the preorogenic basin thickness.

4. Evidence of Basement Control on Development of the Arcuate Belt in NW Taiwan: Transpressional Reactivation of Basement Normal Faults Along the Northern Limb of the Arc

[14] Although the western Taiwan Foothills were considered for a long time as a typical thin-skinned thrust wedge [*Suppe*, 1976, 1980a, 1980b; *Namson*, 1981, 1984], the structure of the frontal units has been recently reinterpreted in terms of superimposed deep-seated (basement) and shallow (cover) decollement tectonics [*Mouthereau et al.*, 2001, 2002; *Lacombe and Mouthereau*, 2002]. These studies emphasize that the variation of the structural style, geometry and regional kinematics of the tectonic wedge along the strike of the Taiwan belt is tightly controlled by the

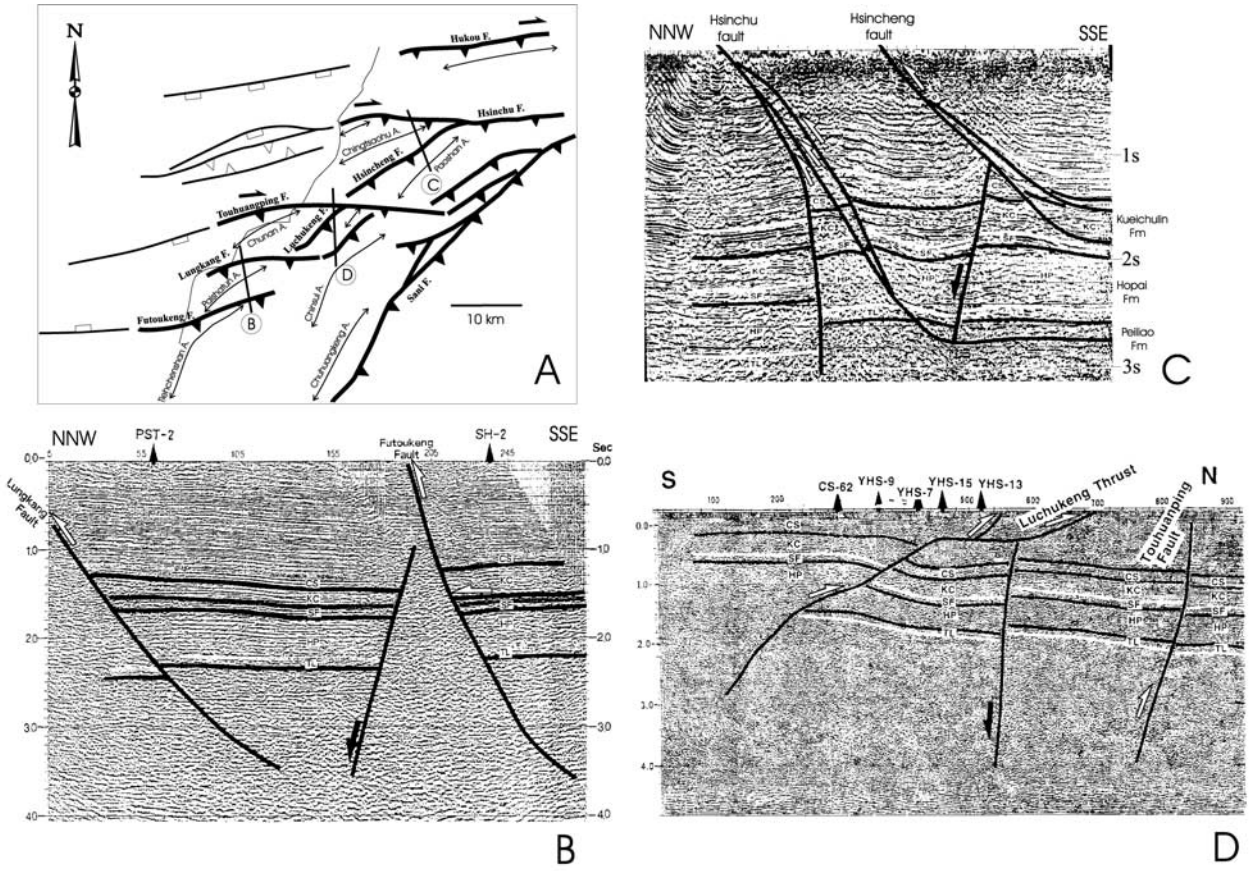

Figure 5. (a) Detailed structural map of the Hsinchu area (location in Figure 2). (b, c, and d) Seismic reflection profiles (location in Figure 5a) after *Yang et al.* [1996] (Figures 5b and 5c) and *Yang et al.* [1997] (Figure 5d). Letters on profiles refer to names of formations of the stratigraphic column of Figure 6.

basement which in some places is involved in collisional shortening, especially on the southern edges of the Peikang and Kuanyin basement highs. We provide hereafter new evidence of basement-involved shortening and reactivation of ancient normal faults inherited from the Chinese margin history (Figures 5 and 6), and we discuss their influence on the development of the NW Taiwan arcuate belt.

4.1. Evidence of Interacting Low-Angle Thin-Skinned Thrust Sheets and Reactivated Normal Faults in NW Taiwan

4.1.1. Northern Part: Hsinchu Area

[15] In the northern part of the salient, field studies as well as seismic reflection profiling reveal two main structural trends (Figure 2). In the offshore Taihsi basin, most features strike N070°, at high angle to the structural grain of the belt: they correspond either to Paleogene to Miocene normal faults which probably extend down to the Mesozoic basement, or to high-angle thrusts which originated from the reactivation of the previous normal faults [*Yang et al.*, 1994, 1997]. The N070° faults extend onshore as south dipping high-angle thrusts (e.g., Hsinchu, Touhuangping, Lungkuang and Futoukeng faults), as shown by seismic lines (Figure 5). Their close association with north and south dipping normal faults, as well as the detailed analysis of thickness and structural elevation of Miocene strata on both sides of the faults [*Yang et al.*, 1996] demonstrate that these high-angle thrusts result from the compressional reactivation of preexisting normal faults of the margin [e.g., *Suppe*, 1984]. Oblique en echelon folds along these high-angle thrusts as well as along-strike variations in magnitude and sense of offset additionally indicate a significant amount of right-lateral wrench movement [*Huang et al.*, 1993; *Lee et al.*, 1993; *Shen et al.*, 1996].

[16] In the inner part of the fold-thrust belt, these high-angle faults connect and/or intersect a system of NNE–SSW folds and low-angle thrusts parallel to the general trend of the belt, such as the Hsincheng and Luchukeng thrusts (Figure 5). Seismic studies show that these low-angle thrusts root within shallow decollement levels (Figure 5) such as the lower-middle Miocene Peiliao and Hopai–Tungkeng formations or the lower Pliocene Kueichulin Formation [*Namson*, 1981, 1984]. In detail, the Hsinchu thrust fault divides into three branches: one is a convex upward high-angle fault that presumably formed from a preexisting normal fault; the

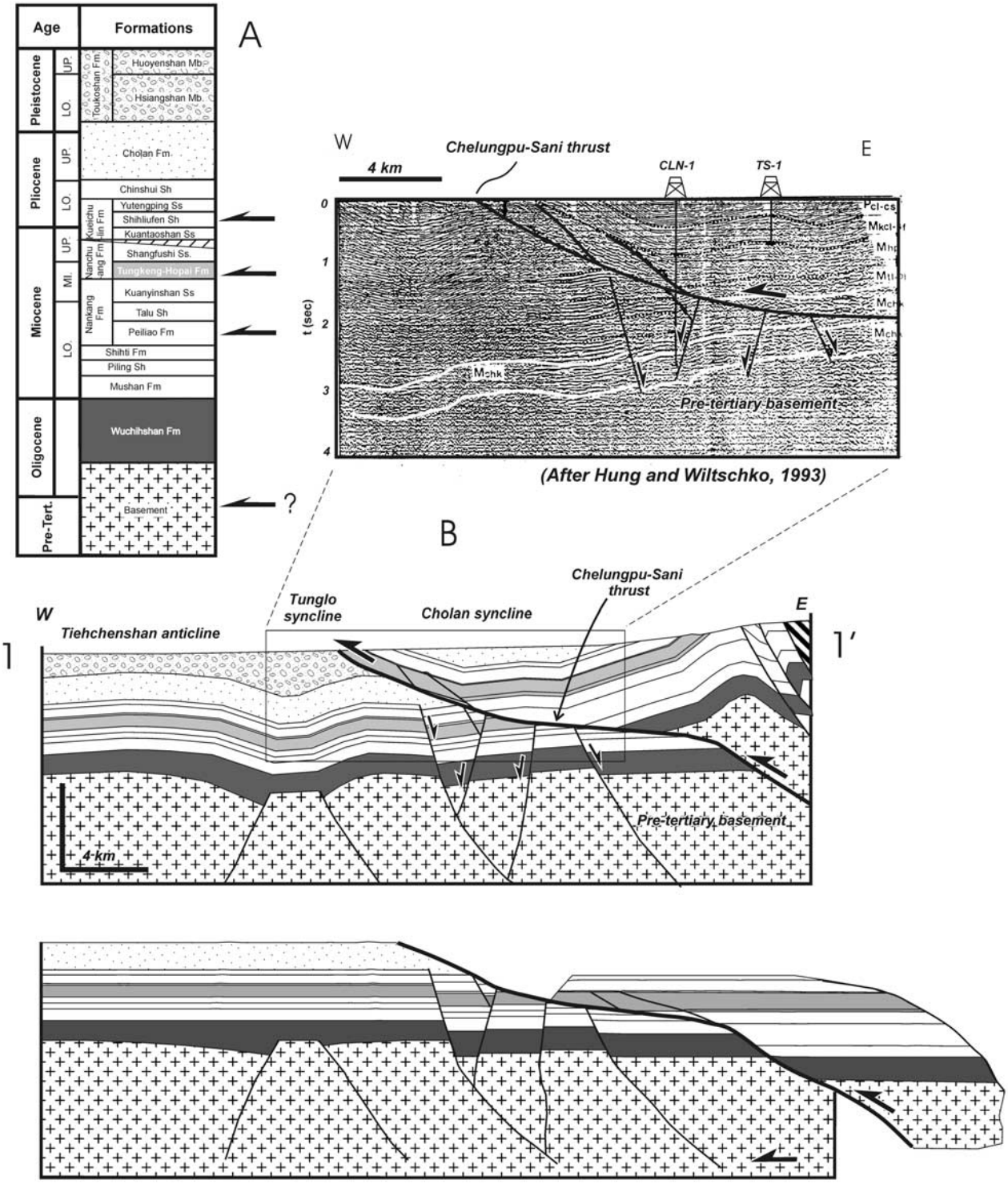

Figure 6. (a) Stratigraphic column of Tertiary formations in NW Taiwan. Arrows indicate potential decollement levels. (b) Geological balanced and restored cross section across the Sani thrust in the Miaoli area (modified after *Mouthereau* [2000]). The frame corresponds to the location of the seismic profile [*Hung and Wiltschko*, 1993]. Note the likely control by ancient normal faults on later compressional deformation.

two other branches change laterally into decollements within the Peiliao formation (Figure 5c). Where the Hsinchu and Hsincheng thrusts faults merge into a single fault, the shallower part of the Hsinchu fault appears as the northern lateral ramp of the Hsincheng thrust. The complex structural pattern of the NW Taiwan belt therefore results from the transpressional reactivation of extensional structures along the southern edge of the Kuanyin basement high which closely interacted with low-angle thrusting.

4.1.2. Central Southern Part: Miaoli Area

[17] The Miaoli area is located at the transition between the thrust system of the Hsinchu area and the northeastern side of the Peikang high (the Taichung area). The main structural feature of the area consists of the Sani thrust, that displays a remarkable bend at 90° angle (Figure 2) and is relayed to the north by the Chuhuangkeng anticline. The balanced cross section of Figure 6 summarizes the structural style of the area. The Sani thrust is made of successive flats and ramps (Figure 6). This geometry is controlled in the western part of the section by a shallow decollement in the Tungkeng Formation; in the eastern part, the thrust extends at depth and presumably roots within a deep detachment level within the basement [e.g., *Lacombe and Mouthereau*, 2002]. The section has been restored with reference to the Chinshui formation which marks the limit between the preorogenic and synorogenic deposits. The restored section suggests that the Sani thrust corresponds to an ancient normal fault of the Chinese margin associated with across-strike changes in the thickness of lower-middle Miocene sediments; we propose that it has been reactivated as a major thrust that cuts through both the cover and the basement.

[18] Accordingly, seismic reflexion data [*Hung and Wiltschko*, 1993] show normal faults cutting through the cover up to the Pliocene Cholan formation (Figure 6): they likely correspond to ancient Miocene normal faults of the margin that were reactivated during the Pliocene in response to the flexure of the foreland during the collision. Unpublished subsurface data (Chinese Petroleum Corporation, personal communication) additionally indicate that the Miocene formations within the Tiehchenshan anticline (Figure 6) are cut by high-angle thrusts and backthrusts that presumably also correspond to inverted ancient normal faults. This suggests that as in the Hsinchu area, the deformation involved significant oblique reactivation of preexisting normal faults, and confirms the conclusions of *Mouthereau et al.* [2002] that both the cover and part of the basement were involved in shortening.

4.2. Quaternary Stress Patterns in NW Taiwan and Evidence of Transpressional Stress Regimes on the Southern Edge of the Kuanyin High

[19] To reconstruct the Quaternary tectonic evolution of the NW Taiwan arcuate belt and to provide constraints on its kinematics, systematic measurements of several hundreds of minor striated faults and extension fractures were carried out within the Miocene to early Pleistocene formations. Inversion of fault slip data was performed using *Angelier*'s [1984] method, which provides the directions of paleostress axes (Figure 7). In addition, within the moderately consolidated conglomeratic formations that poorly record brittle tectonics, we measured the numerous star-like fracture patterns that developed in response to compressional stress and confining pressure where the pebbles of the conglomerates were in contact (Figure 8a). Paleostress analysis was carried out through the statistical interpretation of the orientations of the symmetry axes of such indentation fractures (Figure 8b) which already proved to be a reliable paleostress indicator [e.g., *Lee et al.*, 1996; *Mouthereau et al.*, 1999].

[20] Figure 7 provides examples of the most significant diagrams illustrating fault slip data; the suspected prefolding fault sets were backtilted (backtilting by rotation around the local strike of beds of an amount equal to the bedding dip) and are currently shown in their backtilted attitude (Figures 7l and 7m). Faults display both reverse and strike-slip types. The reverse fault sets are expressed by conjugate small-scale thrust faults and bedding parallel slip planes associated with folds; they may have predated or postdated folding (e.g., Figures 7l, 7f, 7h, and 7k, respectively). The strike-slip fault sets are marked by conjugate strike-slip faults at high angle to bedding: as for the reverse faults, they may have predated or postdated folding (e.g., Figures 7m and 7i, respectively). We conclude that folding and faulting occurred simultaneously, reflecting a dominant synfolding compressional-wrench tectonics.

[21] All fault systems having been found in sedimentary formations whatever their age ranging from Miocene to Pleistocene, accurate stratigraphic constraints on development of fault systems through time were not available. Constraints on tectonic evolution through time are provided by observation of successive slips on fault planes as deduced from crosscutting striations. In many sites of the northern part of the arc, observed superimposed striations on fault planes and stress tensor calculations reveal that fault motions are accounted for by two successive compressions, a N120°E (hereinafter, N120°) compression followed by a N150° to nearly N–S compression (e.g., diagrams f–h and g on Figure 7). Figure 7 illustrates the reconstructed compressional trends gathered with those previously obtained along the northern edge of the Peikang high [*Mouthereau et al.*, 1999] and in the Hsuehshan Range and at the NE tip of the belt [*Angelier et al.*, 1990b; *Lu et al.*, 1995]. Figure 7 shows that in the northern part of the arc, several sites display clear evidence of a tectonic history that involves successive N120° and N150° to N–S compressions (Figure 7), while others only recorded a N150° compression; in contrast, all sites south of 24°30 show a single N100°–120° compression (Figure 7).

[22] Reliable interpretation of these paleostress records requires that careful consideration be paid to block rotations that can be identified from paleomagnetism. Paleomagnetic studies in the area of interest [*Lee et al.*, 1991; *Lue et al.*, 1995; *Lu et al.*, 1995] have revealed clockwise rotations as large as 20°–30° east of the Taipei basin; in contrast, west

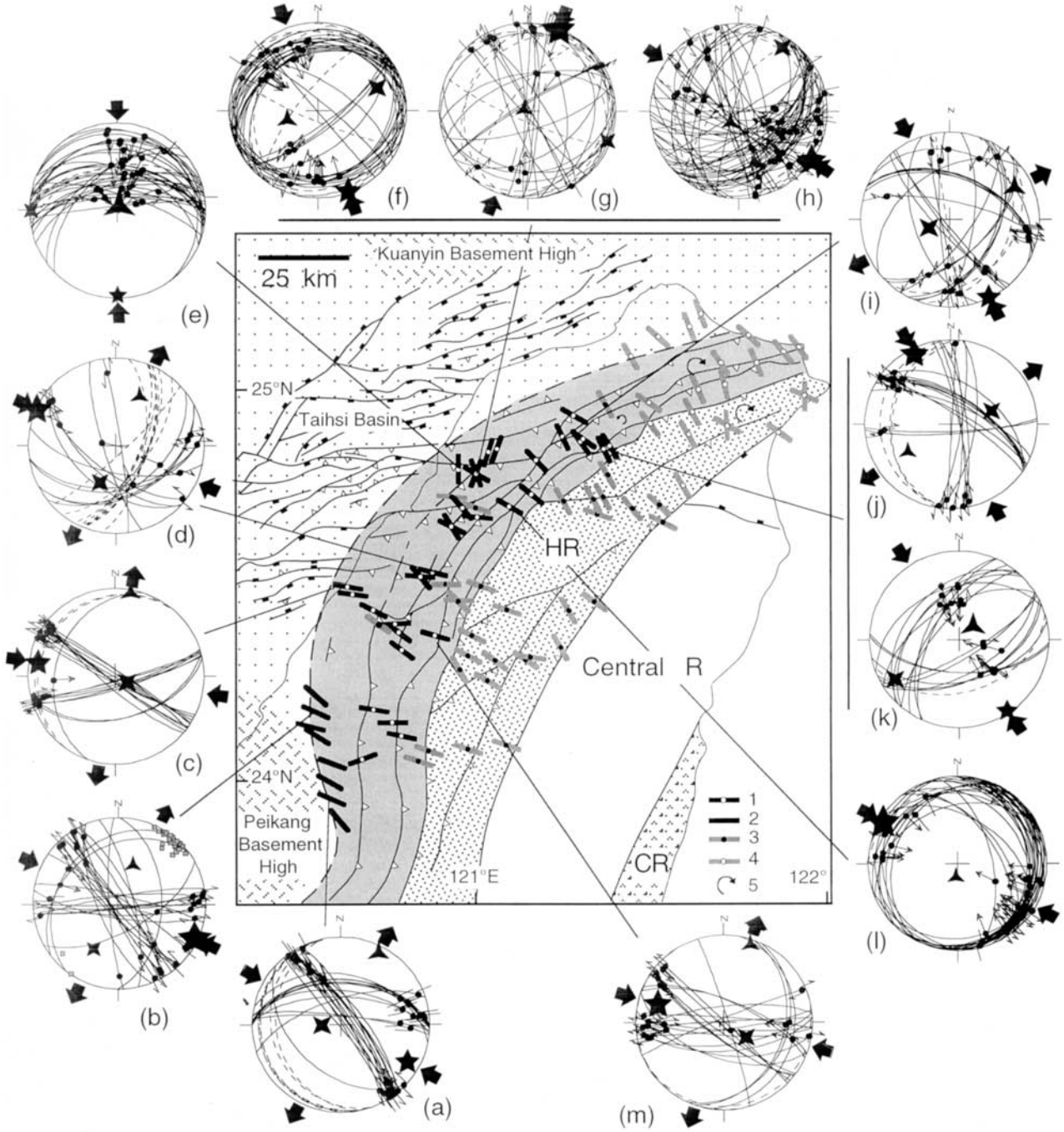

Figure 7. Compression directions deduced from outcrop-scale fault patterns. Dotted pattern: undeformed Chinese margin; Gray pattern: Western Foothills. HR: Hsuehshan Range, Central R.: Central Range, CR: Coastal Range. Diagrams illustrating fault-slip data: thin curves represent fault planes and dots with double arrows (left- or right-lateral) or simple ones (centripetal-reverse) indicate striations. Stars indicate stress axes with five points (σ_1), four points (σ_2) and three points (σ_3). Small gray squares represent poles to tension fractures. Bedding planes shown as dashed lines. Large black arrows: direction of compression (convergent arrows) and extension (divergent arrows); compressional trends on map: 1, this study; 2, after *Mouthereau et al.* [1999]; 3, after *Angelier et al.* [1990b] and *Chu* [1990]; 4, after *Lu et al.* [1995]; 5, vertical axis rotations identified from paleomagnetic studies [*Lee et al.*, 1991; *Lue et al.*, 1995; *Lu et al.*, 1995].

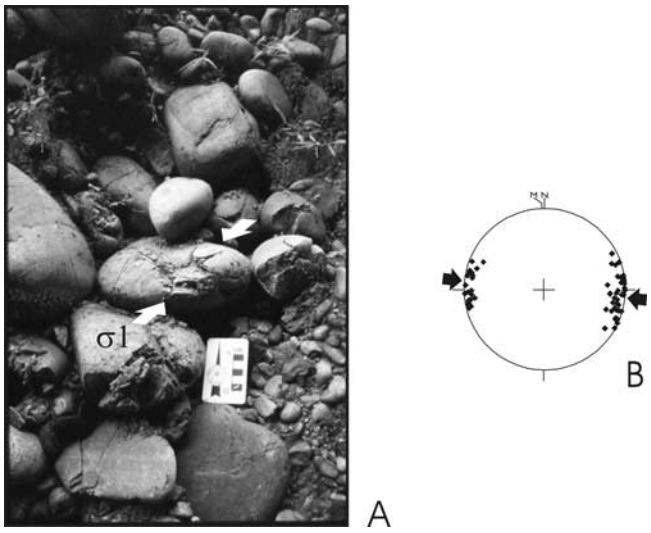

Figure 8. (a) Example of paleostress indicators (star-like features) observed within the conglomerates of the Toukoshan formation. (b) Statistical interpretation of clustering of symmetry axes of star like features (black diamonds) in terms of direction of compression (arrows). Lower hemisphere equal area projection.

of the Taipei basin, rotations are of much lower amounts (less than 10°) and of counterclockwise sense (Figure 7). *Angelier et al.* [1990b] and *Lu et al.* [1995] have interpreted the complex pattern of compressional directions east of the Taipei basin (Figure 7) as partly due to these clockwise block rotations. However, farther west, the N150° and N120° trends of compression are both identified in sites that presumably suffered less than 10° of rotation; so block rotations alone cannot account for occurrence of the two reconstructed compressional trends in the northern part of the arc. We thus propose a regional tectonic history including a N120° compression followed by a N150° to nearly N–S compression. Note that this succession does not require two major tectonic events which are unlikely to have occurred during the short time span considered, and may simply result from a local evolution through time of the regional stress regime in response to the complex kinematics of the collision in NW Taiwan.

[23] Summarizing, the successive paleostress patterns related to the Plio-Pleistocene collision in NW Taiwan can be described as follows. Whereas the first stress regime was dominated by a rather homogeneous direction of compression, N110°–120 on average (Figure 9), the second one was characterized by an asymmetric fan-shaped pattern of directions of compression with strongly divergent orientations: the compressional trends vary from a N120° trend in the central and in southern zones of the arc to N150° and even N–S trends to the north (Figure 9), that is, a fan angle of up to 60°. Although the displacement pattern remains out of reach since it would require a not yet feasible map balancing, an average N120° regional transport direction could be reliably inferred from the trend of regional fold axes, the traces of low-angle thrusts and GPS present-day displacement data [*Yu et al.*, 1997]. In the southern part of the arc, displacement and compression therefore remained coaxial, while to the north the divergence between compression and regional transport suggests significant right-lateral wrench deformation parallel to the N070° trending structures of the margin.

5. Discussion: Kinematic Model of Development of the NW Taiwan Fold-Thrust Belt Salient, and Conclusion

5.1. Kinematics of the Transfer Fault Zones on Both Limbs of the NW Taiwan Arc

[24] During arc formation, basin boundaries often evolve into transfer fault zones that accommodate the contrast in the position of the thrust front resulting from the contrast in sediment thickness. Primary tear faults may thus appear contemporaneously with fold-thrust development, and associated with a curvature of these structures as soon as they form. On both sides, the amount of shortening is the same, but it may be accommodated in a different way. Such a system may secondarily evolve gradually into a transfer (or tear) fault, associated with a clear offset of already formed or currently forming folds, and on both side of which differential displacement/shortening may be accommodated.

[25] The obliquity of the N120° regional transport direction with respect to the orientation of the inherited extensional structures of the margin localized areas dominated by frontal contraction and those dominated by wrench deformation. Frontal contraction occurred against the Peikang high which acted as a buttress for the propagating thrusts [*Lu et al.*, 1998; *Mouthereau et al.*, 1999]. In contrast, the northern edge of the Peikang high as well as the southern edge of the Kuanyin high, which are associated with significant basement offset and changes in thickness of sedimentary formations, have localized conjugate transfer fault zones (or lateral/oblique ramps) that guided the emplacement of the fold-thrust belt and accommodated curvature of the NW Taiwan salient. Wrench deformation which occurs in thrust sheets along the limbs of the salient

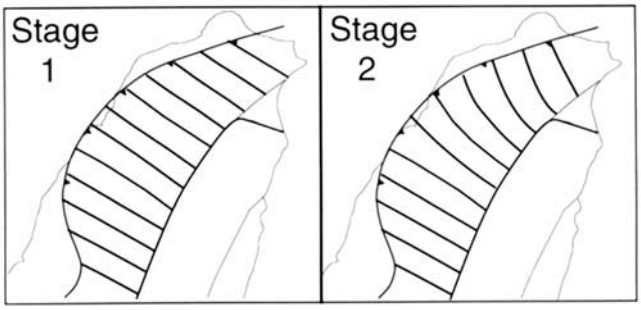

Figure 9. Successive compressional stress patterns during the Pleistocene evolution of NW Taiwan.

(without thrust traces to undergo significant rotation) is due to the oblique motions on such lateral ramps.

5.1.1. Model of Interacting Low-Angle Thrusts and Reactivated Normal Faults in NW Taiwan: Development of a Regional-Scale Oblique Ramp, the Kuanyin Transfer Fault Zone (KTFZ)

[26] During the Pleistocene collisional stage, the N070° to E–W preexisting normal faults of the Taihsi basin evolved in several ways as indicated by seismic data (Figure 5): (1) they became lateral ramp surfaces of low-angle thrust faults, such as the Hsinchu–Hsincheng fault system; (2) they were obliquely inverted and became high-angle thrusts with right-lateral wrench component, such as the Hsinchu, Futoukeng and Lungkang faults; or (3) they were not reactivated and were truncated by shallower thrusts such as in the Paoshan area. The Chingtsaohu anticline (Figure 5a) might have formed first by displacement along the reactivated preexisting normal fault which gave rise to the Hsinchu high-angle thrust, and then cut by the Hsincheng low-angle thrust (Figure 5c), while the shallower part of the Hsinchu fault became the northern lateral ramp of the Hsincheng thrust (Figures 5a and 5c). It can therefore be concluded that the transpressional reactivation of normal faults in the outer belt predated the activation of shallow decollements and related low-angle thrusting in the inner part of the belt as suggested by *Yang et al.* [1996].

[27] Taking into account geometrical, kinematical and time constraints derived from geological maps [e.g., *Chinese Petroleum Corporation*, 1974], seismic data (Figures 5 and 6) and paleostress reconstructions (Figure 7), we propose a coherent scenario of the tectonic and kinematic evolution of the NW Taiwan belt. This scenario, which is depicted in Figure 10, involves the oblique reactivation of the normal faults inherited from the Paleogene-Neogene extensional history of the margin and their interaction with the thrusts of the Plio-Pleistocene Taiwan orogenic wedge which developed in response to the oblique collision of the Chinese margin with the Luzon arc. As Figure 10 suggests, N070° trending normal faults were first obliquely reactivated as high-angle thrusts with right-lateral wrench component in response to the far-field transmission of orogenic stresses during the early stage of the Plio-Pleistocene arc-continent collision. Thrust sheets related to the growing orogenic wedge then initiated in relation to shallow decollement levels in the cover and propagated in a nearly N110–120° transport direction, i.e., obliquely toward the reactivated normal faults, while deforming internally under a nearly uniform N120° compression (Figure 10). In a second stage, the inverted normal faults were used as lateral/oblique ramps for the low-angle thrusts which continued to propagate and consequently turn their strike northward into a direction parallel to the N070° strike of the high-angle thrusts. Our paleostress reconstructions suggest that this second stage was associated with a reorientation of the regional N120° compressional trend which turned into a N150° to N–S trends in the northern part of the arc (Figure 10).

[28] As a result, distributed wrench deformation occurred in the Hsinchu area parallel to the normal faults of the margin. Most of the steeply dipping N070° trending faults show mixed right-lateral and reverse motions, while in most cases the maximum compressive stress is not perpendicular to the fault trend but oblique at high angle. Along the Hsinchu fault the situation is still more complex since N150°, N–S and even N010° compressive trends have been identified from the analysis of minor faults (Figure 7, diagrams f–g–h). At the regional scale, such an obliquity between fault trend and compression suggests that the amount of strike-slip partitioning (the percentage of wrench component imposed by oblique transport direction and accommodated by discrete strike-slip faulting along the N070° trending preexisting structural features) remained low and that transpression prevailed along the southern edge of the Kuanyin high. Following *Teyssier et al.* [1995], the angle α between the trend of the margin faults (N070°) and the regional transport direction (N120°) and the angle β between the trend of the margin faults and the average compression direction (N140°–150°) can be used to estimate the amount of strike-slip partitioning. The corresponding configuration for the Hsinchu area in NW Taiwan is summarized in Figure 10b. The angle α averages 50°, while β can be estimated in the Hsinchu area about 70°–80°, which suggests that the amount of partitioning was probably lower than 50%. The obliquity of the transport direction with respect to the trend of the margin is therefore mainly accommodated by distributed transpression, leading to the development of a regional-scale oblique ramp on the southern edge of the Kuanyin high, the Kuanyin transfer fault zone (KTFZ) (Figure 10).

5.1.2. Kinematics of the Conjugate Pakua Transfer Fault Zone

[29] The southern limb of the arc corresponds to the Pakua transfer fault zone (PTFZ), which accommodated localized wrench deformation along the northern edge of the Peikang high. This transfer fault zone first developed as a primary tear fault above the major normal hinge fault limiting the Peikang basement high to the NE [*Mouthereau et al.*, 1999]. This stage was accompanied by incipient wrench tectonics (conjugate strike-slip faults) in the transverse zone, because of the obliquity between the regional transport direction and the boundary of the high in the undeformed foreland (Figure 11). It secondarily accommodated the differential westward propagation of thin-skinned thrust units along the northern boundary of the Peikang basement high, those in front of the basement high being blocked against it in contrast to the northern units being free to propagate. The blocking induces the activation of out-of-sequence thrust illustrated by the Shuangtung thrust to the east (Figure 11) [*Mouthereau et al.*, 1999]. Local rotation occurred in the southern part with respect to the northern part and induced development of normal faults in the southern Pakuashan area and occurrence of differential slips in the northern part (Figure 11b). This resulted in mesoscale tear faulting, exhibited by en echelon NW trending normal faults associated with wrench deformation in the unconsolidated synorogenic deposits. The transtensional mechanism is superimposed on and parallel to the regional N120° compression. This compression principally induces strike-

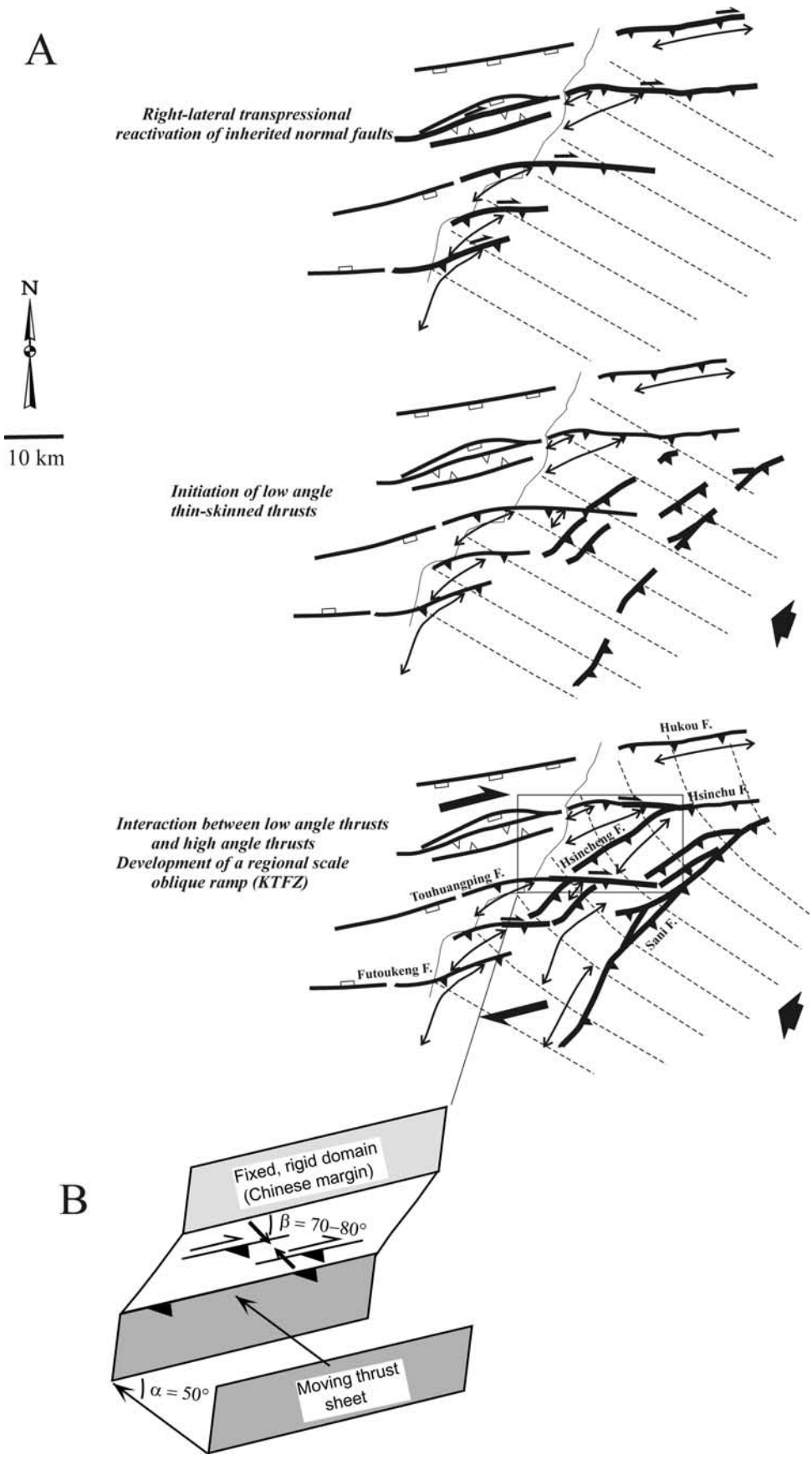
A
Right-lateral transpressional reactivation of inherited normal faults
N
10 km
Initiation of low angle thin-skinned thrusts
Hukou F.
Hsinchu F.
Hsincheng F.
Interaction between low angle thrusts and high angle thrusts
Development of a regional scale oblique ramp (KTFZ)
Touhuangping F.
Futoukeng F.
Sanf F.
B
Fixed, rigid domain (Chinese margin)
β = 70–80°
α = 50°
Moving thrust sheet

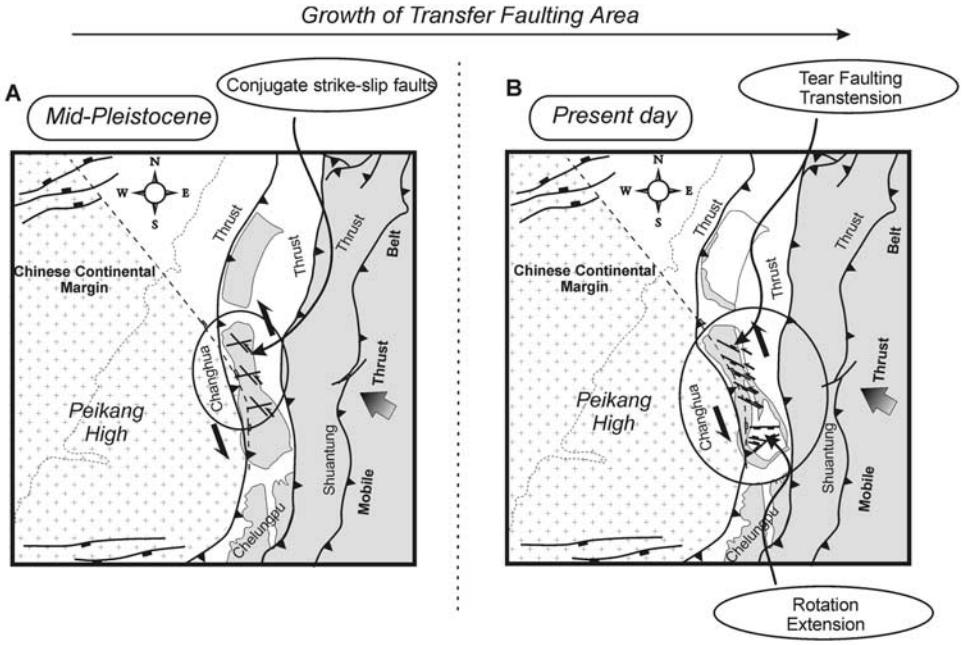

Figure 11. Kinematic and structural model for the development of the Pakua transfer fault zone (modified after *Mouthereau et al.* [1999]). (a) Initial stage. (b) Last stage.

slip faulting because of the relative motion between the transverse zone and the undeformed foreland structure. This stage resulted in the formation of the present-day active Pakua transverse zone. Tear faulting occurred within the transfer zone as observed in the Wyoming Salient [*Apotria*, 1995] or the Wheeler Ridge [*Mueller and Suppe*, 1997], respectively, and allowed frontal curvature of the NW Taiwan salient to be accommodated without creating large divergence between regional transport direction and shortening within the transfer zone (Figures 7 and 9).

5.1.3. Comparison of Geometry and Kinematics of Transfer Fault Zones Bounding the NW Taiwan Belt and Implication for the Asymmetry of the Arc

[30] The N070° Kuanyin transfer fault zone (KTFZ) and the NW trending Pakua transfer fault zone (PTFZ) represent respectively the northern and southern limbs of the NW Taiwan arc along which wrench deformation prevailed (Figure 12). Both fault zones developed in relation with underlying basement boundaries inherited from the extensional history of the margin. These boundaries may correspond either to a single major fault associated with a relatively abrupt variation in thickness of sedimentary formations (on the northern edge of the Peikang high) or a more progressive, normal fault-controlled basement offset and change in thickness of sedimentary formations (on the southern edge of the Kuanyin high). In addition, the orientation of the basin boundaries with respect to the average N120° direction of thrust emplacement is such that transpression and inversion tectonics prevailed along the 070° trending faults bounding the southern edge of the Kuanyin high, while the NW trending Pakua boundary fault on the northern edge of the Peikang high underwent little or no inversion. Together with development of secondary tear faults in the Pakua transfer fault zone [*Mouthereau et al.*, 1999], this accounts for major differences between the conjugate fault zones limiting the NW salient (localized versus distributed wrench deformation and absence versus occurrence of large stress deviations), and therefore for the asymmetry of the salient (Figure 12).

5.2. Development and Kinematics of the NW Taiwan Arc

[31] The NW Taiwan developed in relation to both the oblique impingement of the growing Taiwan wedge by a

Figure 10. (opposite) (a) Kinematic model of interaction between low-angle thrusts and inverted normal faults in the northern part of the NW Taiwan arcuate belt. Dashed lines correspond to compressional stress trajectories derived from microtectonic analyses. The large single arrow corresponds to the regional transport direction of thrust sheets. Heavy black lines underline the faults/thrusts presumably active at each stage. (b) Kinematics of an obliquely moving low-angle thrust sheet toward a fixed rigid domain (the inherited extensional structures of the Chinese margin) in the Hsinchu area. The α is the angle between the trend of the margin faults and the regional transport direction, while β is the angle between the trend of the margin faults and the average shortening direction. The α and β values can be used to estimate the amount of strike-slip partitioning, that is the percentage of wrench component imposed by oblique transport direction accommodated by discrete strike-slip faulting (adapted from *Teyssier et al.* [1995]).

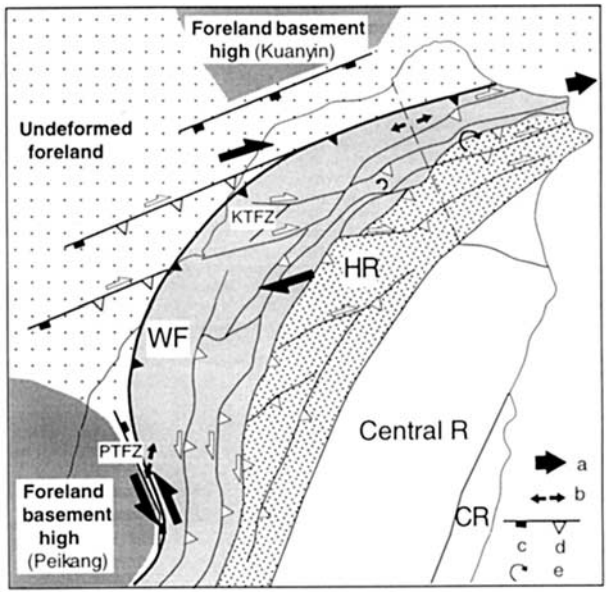

Figure 12. Model of development of the NW Taiwan arcuate belt: The curvature of the basin-controlled salient is accommodated on its southern limb by the Pakua transfer fault zone (PTFZ) and on its northern limb by a diffuse regional-scale oblique ramp (the Kuanyin transfer fault zone, KTFZ) where high-angle wrench-thrust faults inherited from the inversion of normal faults guided the emplacement of thin-skinned low-angle thrusts. WF: Western Foothills; HR: Hsuehshan Range, Central R.: Central Range, CR: Coastal Range. a: tectonic escape at the NE tip of the belt; b: local extension accommodating curvature along the limbs of the arc; c: normal fault of the margin; d: high-angle wrench-thrust fault; e: vertical axis rotations identified from paleomagnetic studies [*Lee et al.*, 1991; *Lue et al.*, 1995; *Lu et al.*, 1995] (see text). Curvature was possibly enhanced at the eastern tip of the belt by the (bulk?) clockwise rotation identified east of the dashed line going through the Taipei basin.

asymmetric hinterland indenter and the irregular shape of the collided Chinese margin. The accreted part of the Luzon arc (the eastern Coastal Range) played the role of the backstop [*Lu and Malavieille*, 1994] while the orientation of the margin as well as its irregular geometry made of promontories and recesses controlled the emplacement and local kinematics of thrust sheets. Even though pushed at the rear by the hinterland indenter, the NW Taiwan arcuate fold-thrust belt is mainly the response to the along-strike variation in the preorogenic basin thickness since it developed in the Taihsi basin where the thickness of preorogenic deposits was greatest. Curvature was therefore achieved at the beginning of the belt formation under a nearly uniform N120° regional transport direction, which strongly argues in favor of a primary arc type.

[32] In terms of geometry, fold trends and thrust strikes (Figure 12) converge toward the end point, in agreement with the lateral thinning of the sedimentary sequence involved in thrusting toward the end points. The NW Taiwan salient therefore mainly formed in response to the along-strike variation in the preorogenic basin thickness, leading to recognize this salient as a basin-controlled salient in the sense of *Macedo and Marshak* [1999]. We rule out the indenter-controlled salient type for which the smallest thrust spacing occurs near the apex because shortening is greater at this locality so trend lines diverge towards the end points [*Macedo and Marshak*, 1999].

[33] The absence of large arc-parallel extension within the outer frontal portion of the arc as deduced from the present study also argues against the "Piedmont glacier" and the orocline types and is in favor of a primary arc type belt [*Marshak et al.*, 1992; *Hindle and Burkhard*, 1999]. Longitudinal extension in a direction nearly parallel to the arc limbs have however been reported: to the south, along the northern edge of the Peikang high, N020–040° extension (Figure 12) has been interpreted as due to the local transtensional kinematics of the Pakua Transfer fault zone [*Mouthereau et al.*, 1999] (Figure 11); to the north, in the Taipei basin, E–W extension (Figure 12) has been related to the bending of the belt at the tip of the hinterland indenter [e.g., *Lu et al.*, 1995]. This last interpretation does not preclude that this extension, limited in amount, may also reflect the nearly arc-parallel extension along arc limbs which is required for accommodating curvature.

[34] The development of the NW Taiwan belt as a primary arc is also supported by the absence of positive evidence for large vertical axis rotations. Despite their scarcity in the southwestern part of the area of interest, the available paleomagnetic data (Figures 7 and 12) show that block rotations presumably did not exceed 10° except for the easternmost part of the northern arc limb, east of the Taipei basin. These rotations therefore remained small with respect to the curvature of the limbs of the arc which describe a 90° angle (Figure 12). Such small rotations together with arc-parallel extension in the limbs of the arc may simply result from simple shear strain due to the oblique motions on lateral ramps even with a uniform displacement, so there is again no need to call out for either significant oroclinal bending, or divergent spreading as in a "Piedmont glacier" type.

[35] Wrench motion along the edges of the basement highs, as deduced from the analysis of the Pakua transfer fault zone [*Mouthereau et al.*, 1999] and the Kuanyin transfer fault zone (this study), suggests a late slight enhancement of curvature by differential westward propagation of the thin-skinned thrust units forming the salient relative to those in front of the basement highs being blocked against them (buttress effect at the end points of the arc). We also do not rule out that curvature has also possibly been enhanced by the 20°–30° clockwise rotation identified at the NE tip of the belt (if the entire area suffered a bulk rotation and did not only undergo local block rotations related to right-lateral strike-slip faults) and which has been related to the late impingement of the wedge by the edge of the hinterland indenter [*Angelier et al.*, 1990b; *Lu et al.*, 1995]; in all cases, this late effect accounts at best

for 20°–30° among the 90° of the fan angle designed by the arc limbs and remained limited to the belt segment east of the Taipei basin.

[36] The NW Taiwan arc is therefore mainly a basin-controlled salient with possible late enhancement of curvature by buttress effects at end points. However, it differs from arcs formed in thin-skinned orogens [*Marshak*, 1988] in that deformation was accommodated by both thin-skinned shallow thrusts and basement faults and therefore that both the cover and the basement are involved in collisional shortening. It additionally differs from more classical primary arcs (if any) in that its rough first-order geometrical symmetry in map view is associated with both a strongly asymmetrical fan-shaped pattern of compressional directions and a strong asymmetrical wrench deformation along its conjugate northern and southern limbs. This study therefore provides new insights into the way arcuate belts may form at obliquely collided irregular margins.

[37] **Acknowledgments.** Fieldwork was supported by the French Institute of Taipei–National Science Council of Taiwan cooperation framework, the Central Geological Survey of Taiwan, and the Academia Sinica. The authors thank the anonymous reviewers for their constructive comments on the manuscript.

References

Angelier, J., Tectonic analysis of fault slip data sets, *J. Geophys. Res.*, *89*(B7), 5835–5848, 1984.

Angelier, J., F. Bergerat, H. T. Chu, W. S. Juang, and C. Y. Lu, Paleostress analysis as a key to margin extension: The Penghu Islands, South China Sea, *Tectonophysics*, *183*, 161–176, 1990a.

Angelier, J. F., F. Bergerat, H.-T. Chu, and T.-Q. Lee, Tectonic analysis and the evolution of a curved collision belt: The Hsuehshan Range, northern Taiwan, *Tectonophysics*, *183*, 77–96, 1990b.

Apotria, T. G., Thrust sheet rotation and out-of-plane strains associated with oblique ramps: An example from the Wyoming salient, USA, *J. Struct. Geol.*, *17*, 647–662, 1995.

Carey, S., The orocline concept in geotectonics, *Proc. R. Soc. Tasmania*, *89*, 255–288, 1955.

Chang, S. S. L., and W. R. Chi, Neogene nannoplankton biostratigraphy in Taiwan and the tectonic implications, *Petrol. Geol. Taiwan*, *19*, 93–147, 1983.

Chinese Petroleum Corporation, Geological maps of Hsinchu and Miaoli, scale 1:10,000, Miaoli City, Taiwan, 1974.

Chou, J. T., A sedimentologic and paleogeographic study of the Neogene formations in the Taichung Region, western Taiwan, *Pet. Geol. Taiwan*, *9*, 43–66, 1971.

Chou, J. T., Stratigraphy and sedimentology of the Miocene in western Taiwan: Pet, *Geol. Taiwan*, *17*, 33–52, 1980.

Chu, H. T., Néotectonique cassante et collision plio-quaternaire à Taiwan: Thèse de Doctorat-ès-Sciences, 292 pp., Univ. Pierre et Marie Curie, Paris, 1990.

Deffontaines, B., O. Lacombe, J. Angelier, H.-T. Chu, F. Mouthereau, C.-T. Lee, J. Deramond, J.-F. Lee, M.-S. Yu, and P.-M. Liew, Quaternary transfer faulting in Taiwan Foothills: Evidence from a multisource approach, *Tectonophysics*, *274*, 61–82, 1997.

Ferrill, D. A., and R. H. Groshong, Kinematic model for the curvature of the northern Subalpine Chain, France, *J. Struct. Geol.*, *15*, 523–541, 1993.

Hindle, D., and M. Burkhard, Strain, displacement and rotation associated with the formation of curvature in fold belt: The example of the Jura arc, *J. Struct. Geol.*, *21*, 1089–1101, 1999.

Huang, S.-T., R.-C. Chen, and W.-R. Chi, Inversion tectonics and evolution of the northern Taihsi basin, Taiwan, *Pet. Geol. Taiwan*, *28*, 15–46, 1993.

Hung, J. H., and D. V. Wiltschko, Structure and kinematics of arcuate thrust faults in the Miaoli Cholan area of western Taiwan, *Pet. Geol. Taiwan*, *28*, 59–96, 1993.

Lacombe, O., and F. Mouthereau, Basement-involved shortening and deep detachment tectonics in forelands of orogens: Insights from recent collision belts (Taiwan, western Alps, Pyrenees), *Tectonics*, *21*(4), 1030, doi:10.1029/2001TC901018, 2002.

Lee, C.-I., Y.-L. Chang, E.-W. Mao, and C. S. Tseng, Fault reactivation and structural inversion in the Hsinchu-Miaoli area of northern Taiwan, *Pet. Geol. Taiwan*, *28*, 47–58, 1993.

Lee, J.-C., C.-T. Lu, H. T. Chu, B. Delcaillau, J. Angelier, and B. Deffontaines, Active deformation and paleostress analysis in the Pakua anticline area of western Taiwan, *Terr. Atmos. Ocean.*, *4*, 431–446, 1996.

Lee, T.-Q., J. Angelier, H.-T. Chu, and F. Bergerat, Rotations in the northeastern collision belt of Taiwan: Preliminary results from paleomagnetism, *Tectonophysics*, *199*, 109–120, 1991.

Lin, A. T., and A. B. Watts, Origin of the West Taiwan basin by orogenic loading and flexure of a rifted continental margin, *J. Geophys. Res.*, *107*(B9), 2185, doi:10.1029/2001JB000669, 2002.

Lu, C. Y., and J. Malavieille, Oblique convergence, indentation and rotation tectonics in the Taiwan Mountain belt: Insights from experimental modelling, *Earth Planet. Sci. Lett.*, *121*, 477–494, 1994.

Lu, C. Y., J. Angelier, H.-T. Chu, and J.-C. Lee, Contractional, transcurrent, rotational and extensional tectonics: Examples from northern Taiwan, *Tectonophysics*, *246*, 129–146, 1995.

Lu, C. Y., F. S. Jeng, K. J. Chang, and W. T. Jian, Impact of basement high on the structure and kinematics of the western Taiwan thrust wedge: Insights from sandbox models, *Terr. Atmos. Ocean*, *9*, 533–550, 1998.

Lue, Y.-T., T.-Q. Lee, and Y. Wang, Paleomagnetic study on the collision-related bending of the fold-thrust belt, northern Taiwan, *J. Geol. Soc. China*, *38*(3), 215–227, 1995.

Macedo, J., and S. Marshak, Controls on the geometry of fold-thrust belt salients, *Geol. Soc. Am. Bull.*, *111*(12), 1808–1822, 1999.

Marshak, S., Kinematics of orocline and arc formation in thin-skinned orogens, *Tectonics*, *7*, 73–86, 1988.

Marshak, S., M. S. Wilkerson, and A. Hsui, Generation of curved fold-thrust belts: Insights from simple physical and analytical models, in *Thrust Tectonics*, edited by K. R. McClay, pp. 83–92, Chapman and Hall, New York, 1992.

Merle, O., Strain models within spreading nappes, *Tectonophysics*, *165*, 57–71, 1989.

Mouthereau, F., Evolution structurale et cinématique récente à actuelle de l'avant-pays plissé d'une chaîne de collision oblique: Taiwan, Ph.D. thesis, 475 pp., Univ. P. et M. Curie, Paris, 2000.

Mouthereau, F., O. Lacombe, B. Deffontaines, J. Angelier, H.-T. Chu, and C.-T. Lee, Quaternary transfer faulting and belt front deformation at Pakuashan (western Taiwan), *Tectonics*, *18*, 215–230, 1999.

Mouthereau, F., O. Lacombe, B. Deffontaines, J. Angelier, and S. Brusset, Deformation history of the southwestern Taiwan foreland thrust belt: Insights from tectono-sedimentary analyses and balanced cross-sections, *Tectonophysics*, *333*, 293–322, 2001.

Mouthereau, F., B. Deffontaines, O. Lacombe, and J. Angelier, Along-strike variations of the Taiwan belt front: Basement control on structural style, wedge geometry and kinematics, *Spec. Publ. Geol. Soc. Am.*, *358*(3), 35–58, 2002.

Mueller, K., and J. Suppe, Growth of Wheeler Ridge anticline, California: Geomorphic evidence for fault-bend folding behavior during earthquake, *J. Struct. Geol.*, *19*, 383–396, 1997.

Namson, J., Detailed structural analysis of the western foothills belt in the Miaoli–Hsinchu area, Taiwan. I: Southern part, *Pet. Geol. Taiwan*, *18*, 31–51, 1981.

Namson, J., Detailed structural analysis of the western foothills belt in the Miaoli-Hsinchu area, Taiwan. III: Northern part, *Pet. Geol. Taiwan*, *20*, 35–52, 1984.

Platt, J. P., J. H. Behrmann, P. C. Cunningham, J. F. Dewey, M. Helman, M. Parish, M. G. Shepley, S. Wallis, and P. J. Weston, Kinematics of the Alpine arc and the motion history of Adria, *Nature*, *337*, 158–161, 1989.

Sengör, A. M. C., Collision of irregular continental margins: Implications for foreland deformation of alpine-type orogens, *Geology*, *4*, 779–782, 1976.

Seno, T., S. Stein, and A. E. Gripp, A model for the motion of Philippine Sea Plate consistent with NUVEL-1 and geological data, *J. Geophys. Res.*, *98*, 17,941–17,948, 1993.

Shaw, C. L., Stratigraphic correlation and isopachs maps of the Western Taiwan Basin, *Terr. Atmos. Ocean*, *7*, 333–360, 1996.

Shen, H.-C., S.-T. Huang, C.-H. Tang, and Y.-Y. Hsu, Geometrical characteristics of structural inversion on the offshore of Miaoli, Taiwan, *Pet. Geol. Taiwan*, *30*, 79–110, 1996.

Sun, S. C., The Tertiary basins of offshore Taiwan: Petroleum geology of Taiwan, in *Petroleum Geology of Taiwan, Proceedings, 2nd Asian Conference on Petroleum* (*ASCOPE*), *Manila, Philippines, 1981*, edited by A. Salivar-Sali, pp. 125–135, Technical Programme Committee, 1982.

Suppe, J., Decollement folding in southwestern Taiwan, *Pet. Geol. Taiwan*, *13*, 25–35, 1976.

Suppe, J., Imbricated structure of western foothills belt, south central Taiwan, *Pet. Geol. Taiwan*, *17*, 1–16, 1980a.

Suppe, J., A retrodeformable cross section of northern Taiwan, *Proc. Geol. Soc. China*, *23*, 46–55, 1980b.

Suppe, J., Mechanics of mountain building and metamorphism in Taiwan, *Mem Geol. Soc. China*, *4*, 67–90, 1981.

Suppe, J., Seismic interpretation of the compressively reactivated normal fault near Hsinchu, western Taiwan, *Pet. Geol. Taiwan*, *20*, 85–96, 1984.

Teng, L. S., Geotectonic evolution of late Cenozoic arc-continent collision in Taiwan, *Tectonophysics*, *183*, 57–76, 1990.

Teyssier, C., B. Tikoff, and M. Markley, Oblique plate motion and continental tectonics, *Geology*, *23*(5), 447–450, 1995.

Yang, K.-M., J. C. Wu, H.-H. Ting, J. B. Wang, and W.-R. Chi, Sequential deformation in foothills belt, Hsinchu and Miaoli areas: Implications in hydrocarbon accumulation, *Pet. Geol. Taiwan*, *29*, 47–74, 1994.

Yang, K.-M., J. C. Wu, J.-S. Wickham, H.-H. Ting, J. B. Wang, and W.-R. Chi, Transverse structures in Hsinchu and Miaoli areas: Structural mode and evolution in foothills belt, northwestern Taiwan, *Pet. Geol. Taiwan*, *30*, 111–150, 1996.

Yang, K.-M., H.-H. Ting, J. C. Wu, and W.-R. Chi, Geological model for complex structures and its implications for hydrocarbon exploration in northwestern Taiwan, *Pet. Geol. Taiwan*, *31*, 1–42, 1997.

Yu, S. B., H.-Y. Chen, and L.-C. Kuo, Velocity field of GPS stations in the Taiwan area, *Tectonophysics*, *274*, 41–59, 1997.

J. Angelier, O. Lacombe, and F. Mouthereau, Laboratoire de Tectonique, UMR 7072, Université P. et M. Curie, T26-25, E1, Boîte 129, 4 pl. Jussieu, F-75252 Paris Cedex 05, France. (jacques.angelier@lgs.jussieu.fr; olivier.lacombe@lgs.jussieu.fr; frederic.mouthereau@lgs.jussieu.fr)

H.-T. Chu, Central Geological Survey, M.O.E.A., P.O. Box 968, Taipei, Taiwan. (chuht@linx.moeacgs.gov.tw)

J.-C. Lee, Institute of Earth Sciences, Academia Sinica, P.O. Box, 1-55, Nankang, Taipei, Taiwan. (jclee@earth.sinica.edu.tw)